

Micromagnetic Simulation of $\text{La}_{0.7}\text{Sr}_{0.3}\text{MnO}_3$ (LSMO) Nano Disk by Finite Element Methods

L. Rohman^{a,b}, I. Sugihartono^{a,c}, W. Nursiyanto^a, D. Djuhana^a, B. Soegijono^a

^aGraduate Program of Material Science, Department of Physics, Faculty Mathematics and Natural Sciences
University of Indonesia, Depok 16424, Tel : (021) 7872610. Fax : (021) 7863441

^bDepartment of Physics, Faculty Mathematics and Natural Sciences
University of Jember 68121, Tel : (0331) 334293. Fax : (0331) 330225

^cDepartment of Physics, Faculty Mathematics and Natural Sciences
State University of Jakarta

E-mail : el_rahman_fmipa@unej.ac.id

Abstract

This researched have been studied the LSMO nanodisk with the various of thicknesses are $t=5\text{nm}$, 10nm and 15nm . The diameter of the nanodisk is constant with the magnitude $D=100\text{nm}$. This researched have done the micromagnetic simulations by finite element method. The finite element method (typically) subdivides space into many small tetrahedra. The tetrahedra are sometimes referred to as the (finite element) mesh elements. While the finite difference method subdivides space into many small cuboids. Finite element simulations are best suited to describe geometries with some amount of curvature, thus the disk (cylindrical) shape is approximated better than with the finite differences. The hysteresis loops shown the barkhausen jump phenomenon in the thickness of nanodisk with $t=15\text{nm}$, $D=100\text{nm}$. This phenomenon relates to the energy profile of the systems. The energy profile of the nanodisk LSMO systems with different thicknesses is dominated by demagnetization energy. This means that the domain structures of the nanodisk are dominated by single domain. The coercive fields of the hysteresis curve are shown the values: 10.5mT , 7.5mT and 1.5mT for the relation to thickness of the nanodisk $t=5\text{nm}$, $t=10\text{nm}$ and $t=15\text{nm}$.

Keywords: *Micromagnetic simulations, LSMO ($\text{La}_{0.7}\text{Sr}_{0.3}\text{MnO}_3$), nanodisk, finite element methods, barkhausen jump, coercivity field, demagnetization energy, and energy profile.*

1. Introduction

LSMO has recently attracted much attention, since perovskite-type manganese oxides exhibit very large magnetoresistance (CMR) and a metal-insulator transition [1]. Curie temperatures (T_c) of LSMO thin films are dependent on strain [2,3], granular structures and granular sizes [4]. A variety of exotic ground states were observed in this materials, for example spin, orbital or charge ordering [5] mediated by possibly cooperative Jahn-Teller distortions, or electronic phase separation [6], as results of the interplay of orbital, spin, charge and lattice degrees of freedom. The strongly correlated characteristic of the manganites and their great potential as spintronics materials for the future application make them one of the hottest topics of solid state physics. Several excellent review articles [6-12] and edited books [13, 14] on manganites are available with different perspective. In our paper we focus our study of magnetic behavior on the LSMO ferromagnetic materials shaped in nano magnetic especially in the nanodisk thin film.

2. Hysteresis and Landau-Lifshitz-Gilbert Equations

Ferromagnetic materials have individual atomic spin moments that interact with each other and align spontaneously in the absence of an external field [15]. This orientation is the same for a small domain, but if we consider a larger sample several small magnetic domains appear and the net magnetization will be approximately zero. The separation between two different magnetic domains represents a domain wall. If an external field is applied, all the magnetic moments tend to align along the direction of the applied field leading to a non-zero net magnetization which is partially maintained when the external field is ceased.

Ferromagnetic materials can be of two types: hard and soft ferromagnets. A soft magnetic is characterized by a narrow hysteresis loop and it is easy to magnetize and to demagnetize. These materials are characterized by high saturation

magnetization M_s , low coercivity H_c and low anisotropy. Hard magnets have high saturation, higher coercivity and high anisotropy which make it difficult to magnetize and demagnetize. Anisotropy refers to the directionality of the magnetization. The magnetic anisotropy energy can be observed when a field is applied in the easy axis direction where a small external field is required to reach saturation, or when the field is applied along the hard axis where a higher field is required.

A typical hysteresis loop is shown in the figure 1.

In order to describe the dynamic response of magnetization to the application of an external magnetic field, the Landau – Lifshitz – Gilbert (LLG) equation is introduced [16, 17].

$$\frac{\partial \mathbf{M}}{\partial t} = -\gamma_G \mathbf{M} \times \mathbf{H}_{eff} + \frac{\alpha}{M_s} \mathbf{M} \times \frac{\partial \mathbf{M}}{\partial t} \quad (1)$$

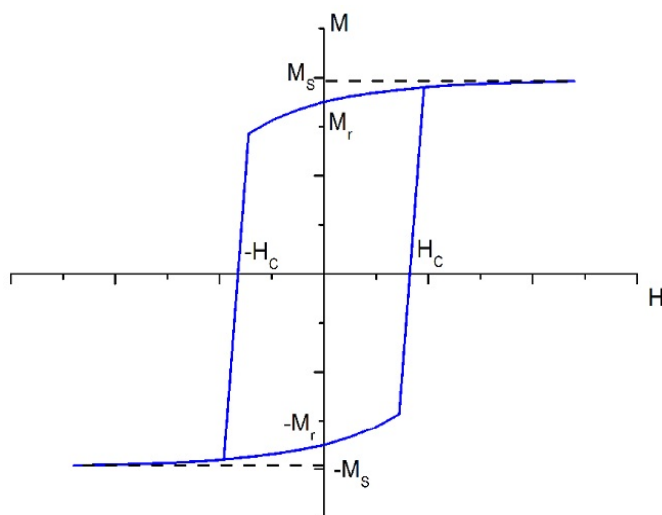


Figure 1. M-H loop for a ferromagnetic material.

3. Micromagnetic Modeling and Simulation Setup

In order to perform the micromagnetic modeling we used the NMAG [18] environment. This program has a collection of Python scripts that runs on a Linux based virtual machine. Some of the important advantages of NMAG are: is based on the finite element method, which is suitable to computing non-cubical structures; problem description is in Python providing a high degree of flexibility; data storage is efficient due to binary compression, and the possibility of extracting it in .vtk [19] files, used further for visualization. To

Where γ_G represents the gyromagnetic constant, H_{eff} is the effective field and α is the damping constant. The first term in the LLG equation represents the precessional part of the dynamics and the second term represents the damping. The effective field is defined as a sum of all the field interacting with the ferromagnet:

$$\mathbf{H}_{eff} = \mathbf{H}_{exch} + \mathbf{H}_d + \mathbf{H}_{ext} + \mathbf{H}_{anis} \quad (2)$$

H_{exch} represents the exchange field, H_d the demagnetizing field, H_{ext} the external applied field and H_{anis} the anisotropy field [16]. Ferromagnetic materials with dimensions in the nanometric region, especially thin films where geometry reduces the demagnetizing field, will form vortices at the crossing points of the domain walls.

define the size and the shape of the structure we used the available primitives from Netgen [20] using finite element mesh generation. Visualization of the .vtk files, which includes dynamic magnetization data, is made by using the Mayavi program [21].

For our simulations we decided to make an analysis on the hysteresis loop for different thickness of disk in the nanometric scale. The chosen physical parameters are characterizing LSMO materials, a soft ferromagnetic which can

be found in [22] and is a commonly used material in the experimental research.

To generate the mesh, we first created the geometry file (.geo) which contains the primitives for developing the desired mesh. By using the geometry file and Netgen v4.4, the desired meshes for our particles was created.

The next step is to make the simulation script using classes and methods from the nmag module. The simulation script has a Python extension (.py) and has a logical and flowing structure. At the beginning of the simulation script we import the nmag module and from this module, we import the SI class used to define physical quantities in SI units, and at class which provides the conditions for saving fields. After the import, we had to set-up the simulation model and to define the magnetic material. Nmag provides the following parameters that can define a magnetic material: name, M_s , llg_damping, llg_gamma_G, exchange_coupling, anisotropy, anisotropy_order and do_precession. For our simulations we defined the LSMO material with M_s is 5.9×10^5 A/m and the exchange stiffness(coupling) is 5×10^{-12} J/m, cubic anisotropy constant is -0.3×10^3 J/m³ with the hard axis is <100> and easy axis is <110>.

Next we had to load the mesh and to define the `unit_length` to scale the mesh. The output file from Netgen is a `.neutral` format, but using `nmeshimport` command we converted it into a `.nmesh.h5` file format. In this case we used the `unit_length` to scale our meshes to the desired dimensions as follows: for the cylinder we used a scaling of 100 nm to obtain a cylinder with 100 nm diameters and 5nm, 10nm and 15nm of thickness.

After the mesh loading, the initial magnetization is defined by a three-dimensional vector in the easy axis direction, as well as by the external field, defined by direction, a normalization vector and the units. In our case we defined the vector for parallel direction to the x-axis or match the desired angles for the applied field 0^0 from x-axis (in-plane of applied field).

The final step of the simulation is to invoke the `sim.hysteresis` method to compute the hysteresis loop and save the required fields. The output is an `.h5` (`hdf5 standard`) format file and stores the time, normalized magnetization, magnetization, total effective field, external field, energy density due to external field, crystal anisotropy field and energy density, exchange field and energy, demagnetization field and energy density, scalar potential for demagnetization field, magnetic charge density and total effective field. To post-process the raw data we must use the `nmagpp` program to convert stored data from `.h5` to `.vtk` files used by Mayavi visualization program. This is done in two steps; first we extract the magnetization field using `nmagpp --dump` command and the second step is actual `.vtk` file creation using `nmagpp --vtk`. Another useful program is `ncol`, used to extract the needed spatial averages fields from the `.ndt` file into a `.dat` or `.txt` file used to plot the hysteresis loop.

4.Simulation Results

The simulations are made on a Debian systems machine running on a 2.4 GHz Intel Core i5-2430M processor with a 6 GB physical memory and 8 GB virtual memory. Each simulation runs on four-core of the processor with parallelization. For every simulation of nanodisk we used the same parameters of the material (parameters colored in red are not be modified):

```

name = LSMO
Ms = <SI: 590000 A / m >
exchange_coupling = <SI: 5e-12 m kg / s^2 >
anisotropy = <function f at 0x28e0500>
anisotropy_order = 4
llg_gamma_G = <SI: 221017 m / s A >
llg_damping = 0.05
llg_normalisationfactor = <SI: 1e+11 / s >
do_precession = True
llg_polarisation = 0.0
llg_xi = 0.0
thermal_factor = <SI: 8.41197e-30 m s A^2 / K >
extended_print = False

```

4.1. Meshing Geometry in The Finite Element Method

To carry out micromagnetic simulations, a set of partial differential equations have to be solved repeatedly. In order to be able to do this, the simulated geometry has to be spatially discretized. The two methods that are most widely spread in micromagnetic modeling are the so-called finite difference (FD) method and the finite element (FE) method. With either the FD or the FE method, we need to integrate the Landau-Lifshitz and Gilbert equation numerically over time (this is a coupled set of ordinary differential equations).

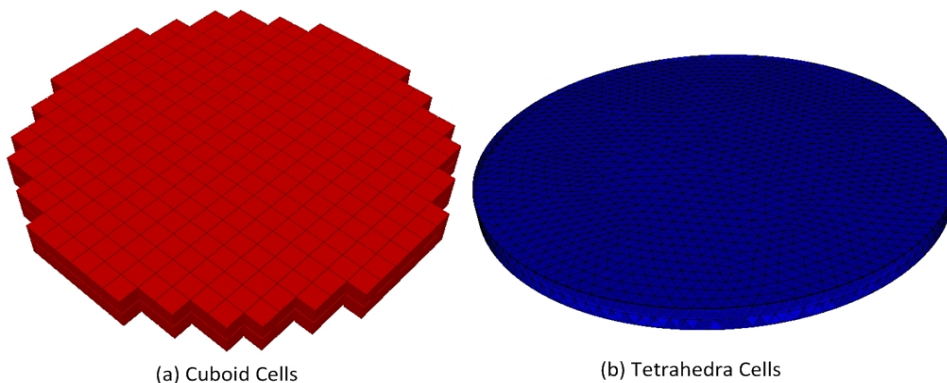


Figure. 2. Approximation of the shape of the disk (a) by cubes and (b) by tetrahedra

The finite difference method subdivides space into many small cuboids. Sometimes the name cell is used to describe one of these cuboids (see fig. 2a). Fig. 2a shows an approximation of the shape of the disk by cubes. This is the finite difference approach. For clarity, we have chosen rather large cubes to resolve the disk – in an actual simulation one would typically use a much smaller cell size in order to resolve geometry better.

The finite element method (typically) subdivides space into many small tetrahedra. The tetrahedra are sometimes referred to as the (finite element) mesh elements. Typically, the geometry of these tetrahedral does vary throughout the simulated region. This allows to combine the tetrahedral to approximate complicated geometries. Fig. 2b shows an approximation of the shape of the disk by tetrahedral. The disk (cylindrical) shape is

approximated better than with the finite differences. Finite element simulations are best suited to describe geometries with some amount of curvature, or angles other than 90 degrees. For such simulations, there is an error associated with the staircase discretization that finite difference approaches have to use. This error is very much reduced when using finite elements.

4.2. Meshing Analysis of Nanodisk Shape and Parallelization (Parmetis)

In this research, there are three sample of nanodisk with three different thicknesses. The analysis of the mesh can do the tools from nmag package systems. The results of the analysis are shown on the table 1.

Table 1. Meshing analysis of three nanodisk size in this researched

t=5nm, D=100nm (scale x 100nm)	t=10nm, D=100nm (scale x 100nm)	t=15nm, D=100nm (scale x 100nm)
3-dimensional mesh 8763 volume elements (3d) 6072 surface elements (2d) 3042 points 1 simplex regions ([1]) 2 point regions ([-1, 1]) 2 region volumes ([0.0, 0.039257686682266264]) 3038 boundary points (-> BEM size<= 70MB) 0 periodic points (mirage=0, total=0) a0: average=0.036797, std=0.013574, min=0.017603, max=0.064580	3-dimensional mesh 33543 volume elements (3d) 6582 surface elements (2d) 7412 points 1 simplex regions ([1]) 2 point regions ([-1, 1]) 2 region volumes ([0.0, 0.07851532959908764]) 3293 boundary points (-> BEM size<= 83MB) 0 periodic points (mirage=0, total=0) a0: average=0.028067, std=0.004822, min=0.014910, max=0.051488	3-dimensional mesh 51311 volume elements (3d) 7212 surface elements (2d) 10588 points 1 simplex regions ([1]) 2 point regions ([-1, 1]) 2 region volumes ([0.0, 0.11777245160578732]) 3608 boundary points (-> BEM size<= 99MB) 0 periodic points (mirage=0, total=0) a0: average=0.027880, std=0.004694, min=0.014886, max=0.051193

Starting from the top of the output of meshing analysis, there are given the information that this is a three-dimensional mesh, with its number of volume elements (i.e. tetrahedra in 3d), surface elements (i.e. surface triangles) and points. There are also given a list of simplex regions (which is just [1] here). If we had more than one region defined (say two disconnected disk that are to be associated with different material), then we would have two entries here. The numbers given in this list are the identifiers of the regions: in this example there is only one region and it has the identifier 1. The point regions is a list of all regions in which points are located. This includes of course region 1. Region -1 represents the vacuum around the meshed region. The points that are located on the surface of the bar are located both in the bar (region 1) and in the vacuum (region -1). The averages lengths of mesh (a0) are

under the exchange length value (4.78 nm).

Nmag's numerical core (which is part of the nsim multi-physics library) has been designed to carry out numerical computation on several CPUs simultaneously. The protocol that we are using for this is the wide spread Message Passing Interface (MPI). There are a number of MPI implementations; the best known ones are probablyMPICH1, MPICH2 and LAM-MPI. In this researched, we have done parallelization of numerical computations by four CPU's on the local machine (MPICH2). For this purpose, we use Metis to partition the mesh. Partitioning means to allocate certain mesh nodes to certain CPUs. Generally, it is good if nodes that are spatially close to each other are assigned to the same CPU. The program MPICH2 starts, and prints the chose partition to stdout for nanodisk t=5nm D=100nm:

```
nmesh.ocaml:2013-03-01 23:04:52,595 INFO
Computing mesh connectivity data
nmesh.ocaml:2013-03-01 23:04:52,711 INFO
Mesh nodes: 3042, simplices: 8763
nfem.ocaml:2013-03-01 23:04:52,712 INFO
Calling ParMETIS to partition the mesh among 4
processors
nfem.ocaml:2013-03-01 23:04:52,750 INFO
Processor 0: 762 nodes
```

```
nfem.ocaml:2013-03-01 23:04:52,751 INFO
Processor 1: 746 nodes
nfem.ocaml:2013-03-01 23:04:52,751 INFO
Processor 2: 783 nodes
nfem.ocaml:2013-03-01 23:04:52,751 INFO
Processor 3: 751 nodes
```

Here we have shown the chosen partition that be done (see Figure. 3).

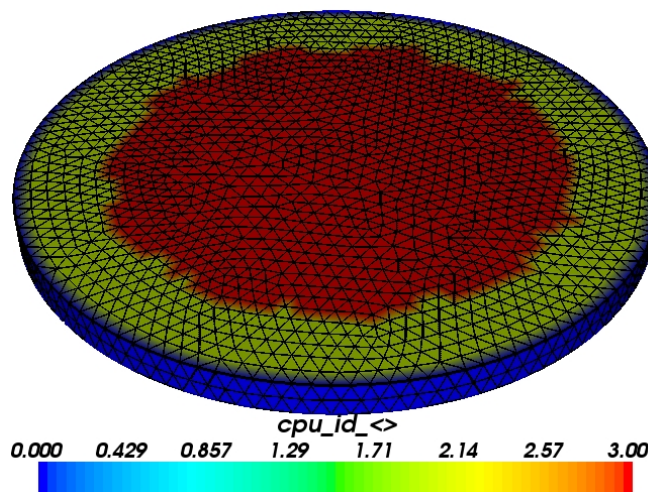


Figure 3. The Disk ($t=5\text{nm}$ $D=100\text{nm}$) has been divided into four areas which carry values 0, 1, 2 and 3 (corresponding to the MPI CPU rank which goes from 0 to 3 for 4 CPUs)

4.3. Magnetic Behaviour of Nanodisk with Different Thicknesses

To analyze how the thicknesses of a nanodisk pattern influences the magnetization we will compare the hysteresis loops for the three thicknesses taken into account, keeping in mind that the diameter disk is kept constant 100nm. The

external magnetic field is applied from 50 mT to -50 mT in any steps on the easy-axis, to apply the external field along the easy axis we used the direction vector (1, 0, 0), like this:

```
Hs = nmag.vector_set( direction=[1.,0.,0.],
norm_list=[0.05, 0.04, [],
0.020,0.019, [],
-0.020, -0.030, [],
-0.05, -0.04, [],
-0.020, -0.019, [],
0.020, 0.030, [], 0.05],
units=si.Tesla/si.mu0 )
```

Figure 4 illustrates the hysteresis loops for all three thicknesses with the external field applied in the direction of the easy-axis. We can see from the figure below that all the hysteresis loops respect the soft ferromagnetic material characteristic. Watching closely we can see that the most optimal thickness with the optimal coercive fields is

$t=10\text{nm}$, no barkhausen jump.

Barkhausen found the first experimental confirmation of the magnetic domain concept in 1919 [23]. He discovered that the magnetization process in an applied field contains discontinuous variations named Barkhausen jumps, which he explained as magnetic domain switching

[Interpretation considered not valid today]. Further analysis of the dynamics of this process [24] led to the conclusion that such jumps can occur by the propagation of the boundary between domains of opposite magnetization.

The coercive fields of the hysteresis curve are shown the values: 10.5 mT, 7.5 mT and 1.5 mT for the relation to thickness of the nanodisk $t=5\text{nm}$, $t=10\text{nm}$ and $t=15\text{nm}$.

4.4. Domain Structure on The Hysteresis Loops

Domain structure of the nanodisk can be figured on the hysteresis loop through the visualization by Mayavi. Figure 5 shows the domain structure of the magnetic domain in the nanodisk with thickness $t=5\text{nm}$, $D=100\text{nm}$. A large saturation field (50 mT) is applied in $-x$ direction (no.1). As the external field is reduced, the spin configuration has no changed (no. 2).

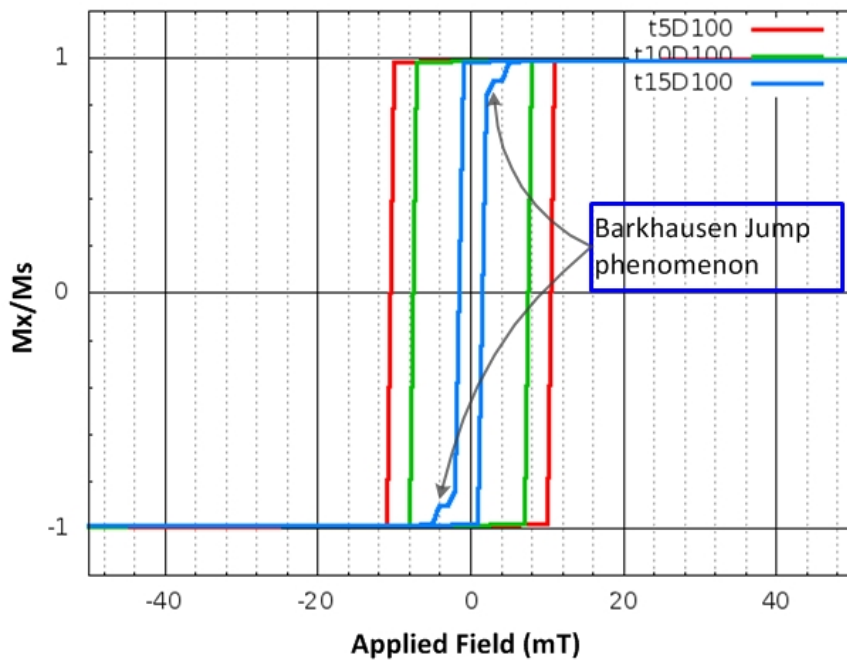


Figure. 4 Hysteresis Curve of different thicknesses of nanodisk pattern in easy-axis external field.

At the point no.2 shows the remanence magnetization that it have a value as same a magnetization saturations. The domain structure shows reversed after the coercivity point. Then, it reached saturation condition (no. 4) that it have the spin configuration opposite to the point number 1. Domain structure of the nanodisk on the other thicknesses has a same configuration as the figure 5.

The energy profile of the nanodisk LSMO systems with different thicknesses is dominated by demagnetization energy. This means that the domain structures of the nanodisk are dominated by single domain. The fluctuations of the profile demagnetization energy and exchange energy on the figure 6(c) related to the barkhausen jump phenomenon.

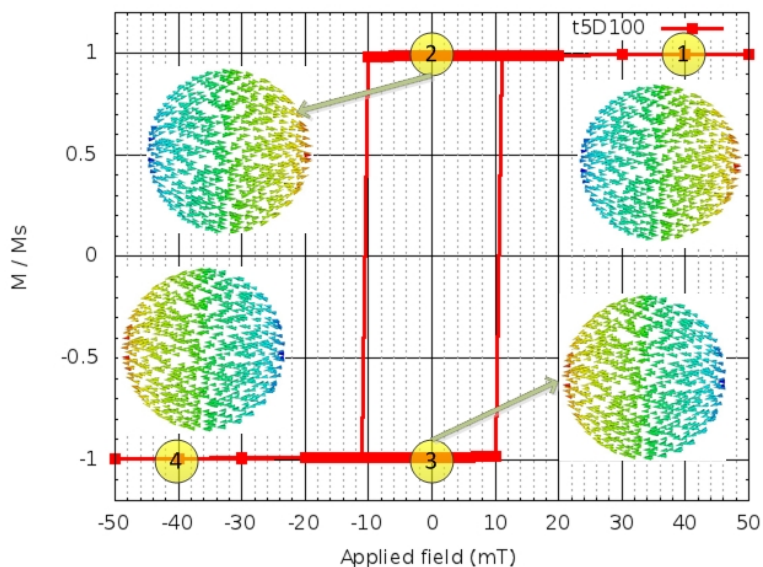


Figure. 5 The domain structure of magnetic domain in the nanodisk with thickness $t=5\text{nm}$, $D=100\text{nm}$.

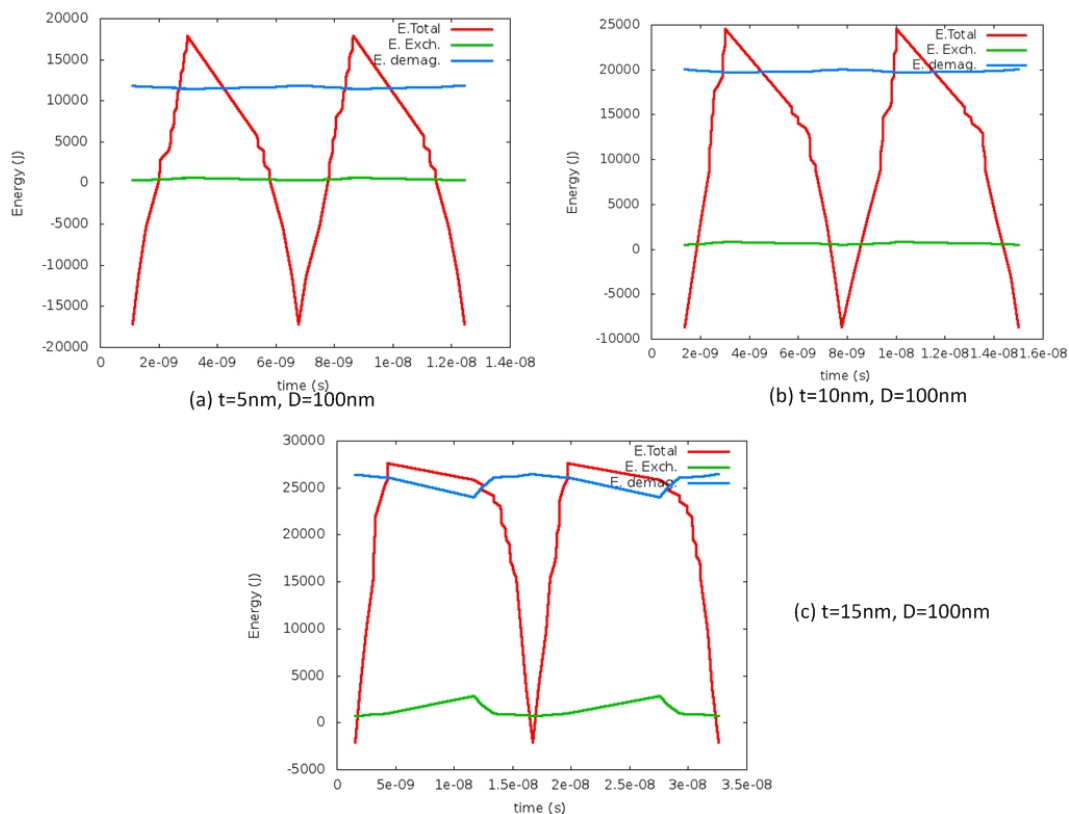


Figure. 6 The energy profile of the nanodisk systems LSMO

5. Conclusions

The evolution of magnetic data storage devices had an exponential development but the current paradigm is reaching the physical limits. In order to improve the existing magnetic data storage devices several non-conventional alternatives have been recently proposed. LSMO is one of several candidate materials need to the researched intensively. The understanding of the LSMO nanodisk especially the magnetic behavior can plays an important role in the development and implementation of these alternatives. This paper shows how the nanodisks of various thicknesses behave in an external magnetic field and the how the characterization of hysteresis loops.

The hysteresis loops shown the barkhausen phenomenon in the thickness of nanodisk with $t=15$ nm, $D=100$ nm. This phenomenon relates to the energy profile of the systems that the profile demagnetization energy and exchange energy are fluctuated.

The energy profile of the nanodisk LSMO systems with different thicknesses is dominated by demagnetization energy. This means that the domain structures of the nanodisk are dominated by single domain.

The coercive fields of the hysteresis curve are shown the values: 10.5 mT, 7.5 mT and 1.5 mT for the relation to thickness of the nanodisk $t=5$ nm, $t=10$ nm and $t=15$ nm.

References

- [1] A. Urushibara, Y. Moritomo, T. Arima, A. Asamitu, G. Kido, Y. Tokura, Phys. Rev. B 51 (1995) 14103.
- [2] Q. Gan, R.A. Rao, J.L. Garret, M. Lee, C.B. Eom, A. Marty, B. Gilles, Mater. Res. Soc. Symp. Proc. 494 (1998) 269.
- [3] A.J. Millis, T. Darling, A. Migliori, J. Appl. Phys. 83 (1998) 1588.
- [4] W.L. Kuang, S.Y. Yang, Y. Liou, S.F. Lee, W.S. Tse, Y.D. Yao, in: Y.-D. Yao, H.-Y. Cheng, C.-S. Chang, S.-F. Lee (Eds.), Proceedings of the Eighth Asia-Pacific Physics Conference, World Scientific, Singapore, 2001, p. 694.
- [5] H. Kuwahara, Y. Tomioka, A. Asamitsu, Y. Moritomo, and Y. Tokura, Science 270, 961 (1995)
- [6] E. Dagotto, T. Hotta, A. Moreo, Phys. Rep. 344, 1 (2001)
- [7] J. Z. Sun and A. Gupta, Annu. Rev. Mater. Sci. 28, 45 (1998)
- [8] J. M. D. Coey, M. Viret, and S. von Molnár, Adv. Phys. 48, 167 (1999)
- [9] W. Prellier, Ph. Lecoeur, and B. Mercey, J. Phys.: Condens. Matter 13, R915 (2001)
- [10] M. B. Salamon, M. Jaime, Rev. Mod. Phys. 73, 583 (2001)
- [11] A. -M. Haghiri-Gosnet and J. -P. Renard, J. Phys. D: Appl. Phys. 36, R127 (2003)
- [12] E. Dagotto, New J. Phys. 7, 67 (2005)
- [13] Colossal Magnetoresistance, Charge Ordering and Related Properties of Manganese Oxides, edited by C. N. R. Rao and B. Raveau, (World Scientific, Singapore, 1998)
- [14] Colossal Magnetoresistive Oxides, edited by Y. Tokura, (Gordon and Breach Science Publisher, Amsterdam, 2000)
- [15] Y. Song and D. Zhu, High density data storage: Principle, Technology, and Materials, World Scientific Publishing, 2009
- [16] H. Kronmuller, S. Parkin, Handbook of Magnetism and Advanced Magnetic Materials, Wiley September 25, 2007.
- [17] R. Antos, YoshiChika Otani, J. Shibata, Magnetic Vortex Dynamics, Journal of the Physical Society of Japan, Vol. 77, No. 3, March, 2008.
- [18] T. Fischbacher, M. Franchin, G. Bordignon, and H. Fangohr, A Systematic Approach to Multiphysics Extensions of Finite-Element-Based Micromagnetic Simulations: Nmag, in IEEE Transactions on Magnetics, 43, 6, 2896-2898 2007.
- [19] <http://www.vtk.org/>
- [20] <http://www.hpem.jku.at/netgen/>
- [21] <http://github.entthought.com/mayavi/mayavi>
- [22] M. Ziese, Phys. Stat. Sol. (b) 243, No.6, 1383-1389 (2006)
- [23] H. Barkhausen, Phys.Z, 20, 401-403, (1919)
- [24] K.J. Sixtus, L.Tonks, Phys.Rev. 37, 930-958 (1931)